Analysis of Hyperbolic Systems for Mobile-Bed, Free-Surface Flow Modelling in Arbitrary Cross Sections

ALBERTO DEPONTI, LUCA BONAVENTURA, LUIGI FRACCAROLLO, EDIE MIGLIO, GIORGIO ROSATTI

MOX, Dipartimento di Matematica "F. Brioschi"
Politecnico di Milano, Via Bonardi 29 - 20133 Milano (Italy)

mox@mate.polimi.it   http://mox.polimi.it

Analysis of Hyperbolic Systems for Mobile–Bed, Free–Surface Flow Modelling in Arbitrary Cross Sections

Alberto Deponti[1], Luca Bonaventura[2], Luigi Fraccarollo[1],
Edie Miglio[2], Giorgio Rosatti[1]

February 20, 2007

[1] CUDAM – Centro Universitario per la Difesa Idrologica dell'Ambiente Montano,
Dipartimento di Ingegneria Civile e Ambientale, Università degli Studi di Trento
Mesiano di Povo, 38050 (TN), Italy
alberto.deponti@ing.unitn.it, giorgio.rosatti@ing.unitn.it,
luigi.fraccarollo@ing.unitn.it

[2] MOX – Modelling and Scientific Computing,
Dipartimento di Matematica "F. Brioschi", Politecnico di Milano
Via Bonardi 9, 20133 Milano, Italy
luca.bonaventura@polimi.it,edie.miglio@polimi.it

Abstract

A model for mobile–bed river hydraulics based on the conservation equations of liquid mass, solid sediment mass and momentum is presented and analysed. The equations are reduced to one dimension by averaging over the cross section. These equations differ from the classical one–dimensional equations for mobile–bed, free–surface flows, since they take into account the effect of non–uniformities in velocity distribution along cross sections of arbitrary shape. By using appropriate closure formulae for sediment transport and for bottom friction, a system of three non–linear hyperbolic equations is obtained. Its eigenstructure is studied and its dependency on the closure formulae and on the non–dimensional parameters determining the flow and transport regimes is investigated. The existence and uniqueness of classical solutions of this hyperbolic system are discussed and an energy inequality for the frozen coefficient problem is derived.

1

1 Introduction

Sediment transport modelling plays a key role in realistic river hydraulic simulations. The morphology of large rivers can change substantially due to sediment transport in areas where accurate prediction of minimum discharge values is essential for environmental planning. For the relevant physical regimes, the inertia and concentration associated to the solid phase is negligible, so that the momentum equation for the solid mass can be disregarded and the solid mass flux assumed to be in local equilibrium with the liquid mass flux. More specifically, the ratio between liquid and solid discharges is assumed to be computable on the basis of various parameters that characterise the flow and the transport regime. This approach is widely used in modelling river flow (see e.g. [1]) and is a key component of state–of–the–art, realistic river flow modelling packages (see e.g. [21]). The resulting equations have been analysed in [4], [12], [19], in the simplified case of sediment transport in a rectangular channel. Modern numerical methods to solve these equations have been proposed e.g. in [3], [5], [8].

The aim of the present work is to extend these analyses to cover the more general case of a section averaged mobile–bed model that allows for sections of arbitrary shape, as for example in [21]. This should provide a sound mathematical background for the derivation of advanced numerical methods that can be useful for realistic applications. In particular, the present work is motivated by a research project aimed at the development of a multi–scale model of the river Adige (Italy), to be used for environmental management purposes. The aim of the project is the development of a mobile–bed, free–surface model based on the 1D–2D coupling technique proposed in [14], [15] that allows for long time range and high resolution realistic simulations at the lowest possible computational cost. A key step in performing this extension is to ensure that the classical results available for the fixed–bed, rectangular section channel flow equations are also valid in the mobile–bed, variable cross section case.

In this paper, the hyperbolic system of the section averaged model will be fully analysed. Its eigenvalues and eigenvectors will be derived, highlighting their dependency on non–dimensional parameters related to the section shape and to the sediment transport regime. The choice of the primitive variables is different from the purely one–dimensional case and is consistent with the need of equation averaging over arbitrary cross section geometries. By doing so and by exploiting a properly defined Froude number, the study of the eigenstructure is applicable to a realistic setting, while recovering the classical results relevant to simple channel geometries. The novel findings provide further insights on the important issue of possible decoupling between hydro– and morphodynamics. Finally, the appropriate boundary conditions will be derived in order to achieve existence and uniqueness of classical solutions for small perturbations of steady state flows and to guarantee the validity of an energy inequality for the linearised, frozen coefficient problem.

The paper is organised as it follows. In section 2, the conservation equations for liquid mass, solid mass and momentum, valid for relatively small sediment concentration, are described, as formulated in most sedi-

ment transport models used in hydraulic engineering. In section 3, some closure formulae widely used to parameterise the solid discharge in local equilibrium are briefly reviewed and presented in a coherent framework, as convenient for a comprehensive mathematical analysis. In section 4 the structure of the eigenvalues of the associated hyperbolic systems is analysed as a function of the different flow and transport regimes. In section 5, the corresponding eigenvector structure is described. In both cases, the differences with the much better known rectangular cross section case are highlighted. A qualitative analysis of the solution behaviour in the different flow and transport regimes is carried out in section 6. The full derivation of the eigenstructure is reported in the appendix. In section 7, boundary conditions are discussed, that guarantee existence and uniqueness of classical solutions and an energy inequality for the linearised, frozen coefficient problem is presented.

2 The section–averaged equations for mobile–bed, free–surface channel flow

The section–averaged equations for mobile–bed, free–surface channel flow (see e.g. [1]) can be written

$$\frac{\partial A_l}{\partial t} + \frac{\partial Q_l}{\partial x} = 0, \tag{1}$$

$$\frac{\partial Q_l}{\partial t} + \frac{\partial}{\partial x}\left(\beta\frac{Q_l^2}{A_l}\right) + gA_l\frac{\partial \eta}{\partial x} = -\frac{\bar{\tau}_0}{\rho}C_w, \tag{2}$$

$$\frac{\partial A_s}{\partial t} + \frac{\partial Q_s}{\partial x} = 0. \tag{3}$$

Here, A_l denotes the liquid area of the cross section (i.e., the area occupied by water), A_s denotes the area of the cross section occupied by sediment in a frame of reference, η is the height of the water surface above a fixed reference level, g is the gravity acceleration, Q_l the liquid discharge, Q_s the solid discharge divided by $(1 - p)$, p being the sediment porosity, $\bar{\tau}_0$ the average bottom friction, ρ the water density, and C_w the length of the wet contour (see figure 1 for a sketch of the generic cross section). In this work, arbitrarily shaped cross sections are considered, that can have geometries like those found in nature. The only assumptions are that multiple channels are not considered and that the liquid area of the cross section is a monotonic function of the surface elevation so that $\partial A_l/\partial \eta \geq 0$. The Coriolis averaging coefficient β in the momentum conservation equation (2), takes into account the effects due to the two dimensional variability of the axial velocity u across the section and is defined by

$$\beta = \frac{1}{A_l}\int_{A_l}\frac{u^2}{U^2}dA_l. \tag{4}$$

where U is the averaged velocity.

Equations (1)–(3) express the conservation of liquid mass, momentum and solid mass. These equations are valid for $Q_s \ll Q_l$ [19]. In general, the

3
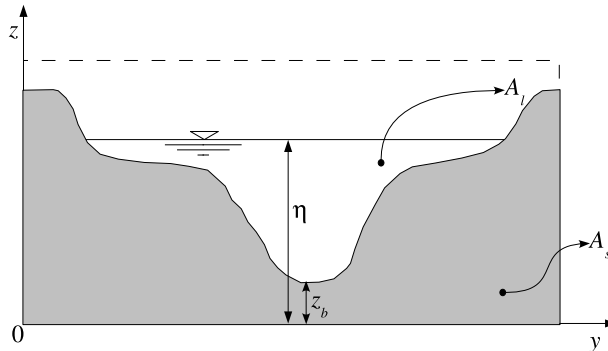
Figure 1: Sketch of a generic cross section and of the main model variables.

liquid area and the Coriolis coefficient can be expressed as functions $A_l = A_l(\eta, A_s)$, $\beta = \beta(\eta, A_s)$ depending on the free surface height and on the solid area. If a local equilibrium assumption is made (see the discussion in section 3), the ratio between the solid and liquid discharge can be expressed as a function of bulk properties of the flow and sediment as

$$\Psi = \frac{Q_s}{Q_l} = \Psi(U, d, \Delta, \rho, \rho_s, \eta, Q_l, A_s). \tag{5}$$

Here d is the sediment diameter, ρ and ρ_s water and sediment density respectively, $\Delta = (\rho - \rho_s)/\rho$ the sediment relative density. Some alternatives for the precise form of Ψ will be discussed in the following. Here we will simply remark that using the general closure formula (5) equation (3), can be rewritten as

$$\frac{\partial A_s}{\partial t} + \frac{(\partial \Psi Q_l)}{\partial x} = 0. \tag{6}$$

The prognostic variables of the model are η, Q_l, A_s, while the other quantities are recovered using closure formulae. It worths noticing that the choice of the prognostic variables is different from classical one–dimensional models. In the latter, indeed, the prognostic variables are usually surface elevation η or water depth h, mean velocity U and the elevation of the lower point of the bottom z_b (see figure 1). While Q_l is equivalent to U, A_s and z_b are deeply different; the solid area A_s is an averaged quantity and carries information related to the cross section geometry while the hight of the lowest point of the bottom z_b is a point variable; the use of z_b in a section–averaged model would lead to a lack of information related to cross section geometry.

In order to analyse the eigenstructure of the system made up by equations (1), (2) and (6), we rewrite the equations applying the chain rule

4

as

$$\left(\frac{\partial A_l}{\partial \eta}\right)\frac{\partial \eta}{\partial t} + \left(\frac{\partial A_l}{\partial A_s}\right)\frac{\partial A_s}{\partial t} + \left(\frac{\partial Q_l}{\partial x}\right) = 0, \tag{7}$$

$$\frac{\partial Q_l}{\partial t} + \left(\frac{Q_l^2}{A_l}\frac{\partial \beta}{\partial \eta} - \frac{\beta Q_l^2}{A_l^2}\frac{\partial A_l}{\partial \eta} + gA_l\right)\frac{\partial \eta}{\partial x} + \left(\frac{2\beta Q_l}{A_l}\right)\frac{\partial Q_l}{\partial x} +$$
$$+ \left(\frac{Q_l^2}{A_l}\frac{\partial \beta}{\partial A_s} - \frac{\beta Q_l^2}{A_l^2}\frac{\partial A_l}{\partial A_s}\right)\frac{\partial A_s}{\partial x} = -\frac{\bar\tau_0}{\rho}C_w, \tag{8}$$

$$\frac{\partial A_s}{\partial t} + \left(Q_l\frac{\partial \Psi}{\partial \eta}\right)\frac{\partial \eta}{\partial x} +$$
$$+ \left(\Psi + Q_l\frac{\partial \Psi}{\partial Q_l}\right)\frac{\partial Q_l}{\partial x} + \left(Q_l\frac{\partial \Psi}{\partial A_s}\right)\frac{\partial A_s}{\partial x} = 0. \tag{9}$$

The resulting system can be written in matrix form as

$$\mathbf{B}\frac{\partial \mathbf{U}}{\partial t} + \mathbf{A}\frac{\partial \mathbf{U}}{\partial x} = \mathbf{S} \tag{10}$$

where we have defined

$$\mathbf{U} = \begin{bmatrix} \eta \\ Q_l \\ A_s \end{bmatrix}, \quad \mathbf{B} = \begin{bmatrix} \left(\frac{\partial A_l}{\partial \eta}\right) & 0 & \left(\frac{\partial A_l}{\partial A_s}\right) \\ 0 & 1 & 0 \\ 0 & 0 & 1 \end{bmatrix}, \quad \mathbf{S} = \begin{bmatrix} 0 \\ -\frac{\bar\tau_0}{\rho}C_w \\ 0 \end{bmatrix},$$

$$\mathbf{A} = \begin{bmatrix} 0 & 1 & 0 \\ \left(\begin{array}{c} \frac{Q_l^2}{A_l}\frac{\partial \beta}{\partial \eta} + \\ -\frac{\beta Q_l^2}{A_l^2}\frac{\partial A_l}{\partial \eta} + gA_l \end{array}\right) & \left(\frac{2\beta Q_l}{A_l}\right) & \left(\begin{array}{c} \frac{Q_l^2}{A_l}\frac{\partial \beta}{\partial A_s} + \\ -\frac{\beta Q_l^2}{A_l^2}\frac{\partial A_l}{\partial A_s} \end{array}\right) \\ \left(Q_l\frac{\partial \Psi}{\partial \eta}\right) & \left(\Psi + Q_l\frac{\partial \Psi}{\partial Q_l}\right) & \left(Q_l\frac{\partial \Psi}{\partial A_s}\right) \end{bmatrix}$$

If no lateral bank breaks occur, then surface width depends on surface elevation only and $\partial A_l/\partial A_s = -1$; moreover, for simplicity in the following analysis we consider $\beta = 1$.

3   Sediment transport closure formulae

Several sediment transport closure formulae are available in the literature. A complete treatment of the topic is beyond the target of the present work; here we just mention some examples.

The simplest transport formula is based on the assumption that the ratio $\Psi = Q_s/Q_l$ can be expressed as a power of the mean velocity and water depth: $\Psi = a_s U^m h^n$, where a_s is a constant depending on cross section geometry and on the nature of the sediment, m and n are two exponents. A good choice for the exponents is $m = 2$ and $h = -1$ leading to [1]:

$$\Psi = a_s \frac{U^2}{h} \tag{11}$$

Other monomial formulas are based on the Shields mobility parameter define by:

$$\theta = \frac{Q_l^2}{A_l^2 \chi^2 d\Delta},$$

(12)

where χ is Chézy roughness parameter. Two examples are the Einstein–Brown formula [6], [2]:

$$\Psi = \frac{100Bd\sqrt{gd\Delta}\theta^3}{Q_l}$$

(13)

and the Engelund–Hansen formula [7]:

$$\Psi = \frac{0.084Bd\sqrt{gd\Delta}\theta^{5/2}}{Q_l}$$

(14)

where B is the surface width.

A more complicated example of monomial formula is the Parker formula [17], defined by:

$$\Psi = 0.00218Bd\sqrt{gd\Delta}\left(\frac{\theta^{\frac{3}{2}}}{Q_l}G\left(\xi\right)\right),$$

(15)

where $\xi = \theta/0.0386$ and

$$G(\xi) = \begin{cases} 5471\left(1 - \dfrac{0,853}{\xi}\right)^{4.5} & if \quad \xi > 1.65\,, \\ \exp\left[14.2\left(\xi - 1\right) - 9.28\left(\xi - 1\right)^2\right] & if \quad 1 < \xi \le 1.65\,, \\ \xi^{14.2} & if \quad \xi \le 1\,. \end{cases}$$

(16)

The Meyer–Peter and Müller formula [13] is an example of a formula that use a threshold below which no sediment transport occurs. It can be written as:

$$\Psi = \begin{cases} \dfrac{8Bd\sqrt{gd\Delta}\left(\theta - \theta_c\right)^{3/2}}{Q_l} & if \quad \theta > \theta_c \\ 0 & if \quad \theta \le \theta_c \end{cases}$$

(17)

The threshold value θ_c is, in general, non–constant, depending on the physical properties of the sediment, on the channel shape and on the flow regime; nevertheless, in most real applications where the bed inclination is not too large, the sediment size is homogeneous and the turbulence is fully developed, the value 0.047 is usually considered.

4 Eigenvalues of the hyperbolic systems for mobile–bed, free–surface channel flow

The characteristic polynomial $p\left(\lambda\right)$ associated to system (10) has been computed in order to study the behaviour of the eigenvalues as functions of the different flow and transport regimes and different cross section geometries. The algebra is quite cumbersome, so that the complete derivation

is reported in the appendix. After rescaling by $\left[\left(-\frac{\partial A_l}{\partial \eta} \right)^{-1} \left(\frac{1}{gA_l} \frac{\partial A_l}{\partial \eta} \right)^{2/3} \right]$, and defining the non–dimensional eigenvalues

$$\mu = \lambda \sqrt{\frac{1}{gA_l} \frac{\partial A_l}{\partial \eta}} \tag{18}$$

and the generalised Froude number

$$\mathrm{Fr} = \sqrt{\frac{Q_l^2}{gA_l^3} \frac{\partial A_l}{\partial \eta}}, \tag{19}$$

the non–dimensionalised characteristic polynomial takes the form

$$p(\mu) = b_3 \mu^3 + b_2 \mu^2 + b_1 \mu + b_0, \tag{20}$$

where the coefficients are given by

$$
\begin{aligned}
b_0 &= 3\Theta\Phi\Psi\,\mathrm{Fr} & (21) \\
b_1 &= \mathrm{Fr}^2 - 1 - 3\Theta\Psi & (22) \\
b_2 &= -2\,\mathrm{Fr} & (23) \\
b_3 &= 1 & (24)
\end{aligned}
$$

Here Φ is a shape parameter depending on the section geometry and Θ is a mobility parameter depending on the physical characteristics of the sediment. Since the coefficients (21)–(24) in formula (20) only depend on non–dimensional parameters, it is possible to analyse the dependency of the eigenstructure of system (10) on different cross section geometries and different flow and sediment transport regimes. For example, the sediment transport parameter Ψ is zero for the fixed–bed case while it is non–zero for mobile–bed cases. The shape parameter Φ is equal to one in the case of rectangular cross section and monomial transport formula while it is larger then one for different cross section geometries or different transport formulae. The mobility parameter Θ is equal to one for the monomial formula while it is equal to $\theta/(\theta - \theta_c)$ for the Meyer–Peter and Müller formula. Typical values for the shape parameter Φ are 1.1–1.5 for compact cross sections and 1.5–2.0 for non–compact cross sections. In table 1 the values of the parameters describing the system eigenstructure are summarised for different geometries and different sediment transport formulae.

In the case of fixed–bed flow, it is customary to fix the value of the sediment transport and to analyse the behaviour of the eigenvalues by plotting their values as functions of the Froude number (see e.g. [1] and [19]). In the case of mobile–bed flow, it is possible to fix the values of the three parameters Φ, Ψ and Θ and plot the eigenvalues as functions of the generalised Froude number. Strictly speaking, parameters Ψ and Θ depend on the Froude number, so that the choice of keeping them fixed is just a simplification that helps in performing a simple analysis. It would be possible to consider the dependency of Ψ and Θ on the Froude number; this would lead to variations and asymmetries in the system eigenstructure that are larger than those presented in the forthcoming results. It has to be remarked that

Monomial Formula

$$\Psi = a_s \frac{U^2}{h} \qquad \Theta = 1$$

Rectangular Section	Arbitrary Section
$\Phi = 1$	$\Phi = \dfrac{1}{3}\left(2 - \dfrac{A_l}{h}\dfrac{\partial h}{\partial A_s}\right)$
$\mu = \dfrac{\lambda}{\sqrt{gh}}$	$\mu = \lambda\sqrt{\dfrac{1}{gA_l}\dfrac{\partial A_l}{\partial \eta}}$
$\mathrm{Fr} = \dfrac{U}{\sqrt{gh}}$	$\mathrm{Fr} = \sqrt{\dfrac{Q_l^2}{gA_l^3}\dfrac{\partial A_l}{\partial \eta}}$

Meyer–Peter and Müller Formula

$$\Psi = \begin{cases} \dfrac{8Bd\sqrt{gd\Delta}\,(\theta - \theta_c)^{3/2}}{Q_l} & if \quad \theta > \theta_c \\ 0 & if \quad \theta \le \theta_c \end{cases}$$

$$\Theta = \frac{\theta}{\theta - \theta_c}$$

Rectangular Section	Arbitrary Section
$\Phi = \left[1 + \dfrac{B}{6\,(B+2h)}\right]$	$\Phi = \left[1 - \dfrac{C_w}{6}\dfrac{\partial R_h}{\partial h}\dfrac{\partial h}{\partial A_s}\right]$
$\mu = \dfrac{\lambda}{\sqrt{gh}}$	$\mu = \lambda\sqrt{\dfrac{1}{gA_l}\dfrac{\partial A_l}{\partial \eta}}$
$\mathrm{Fr} = \dfrac{U}{\sqrt{gh}}$	$\mathrm{Fr} = \sqrt{\dfrac{Q_l^2}{gA_l^3}\dfrac{\partial A_l}{\partial \eta}}$

Table 1: Values of the parameters governing the system eigenstructure for different geometries and different transport formulae.
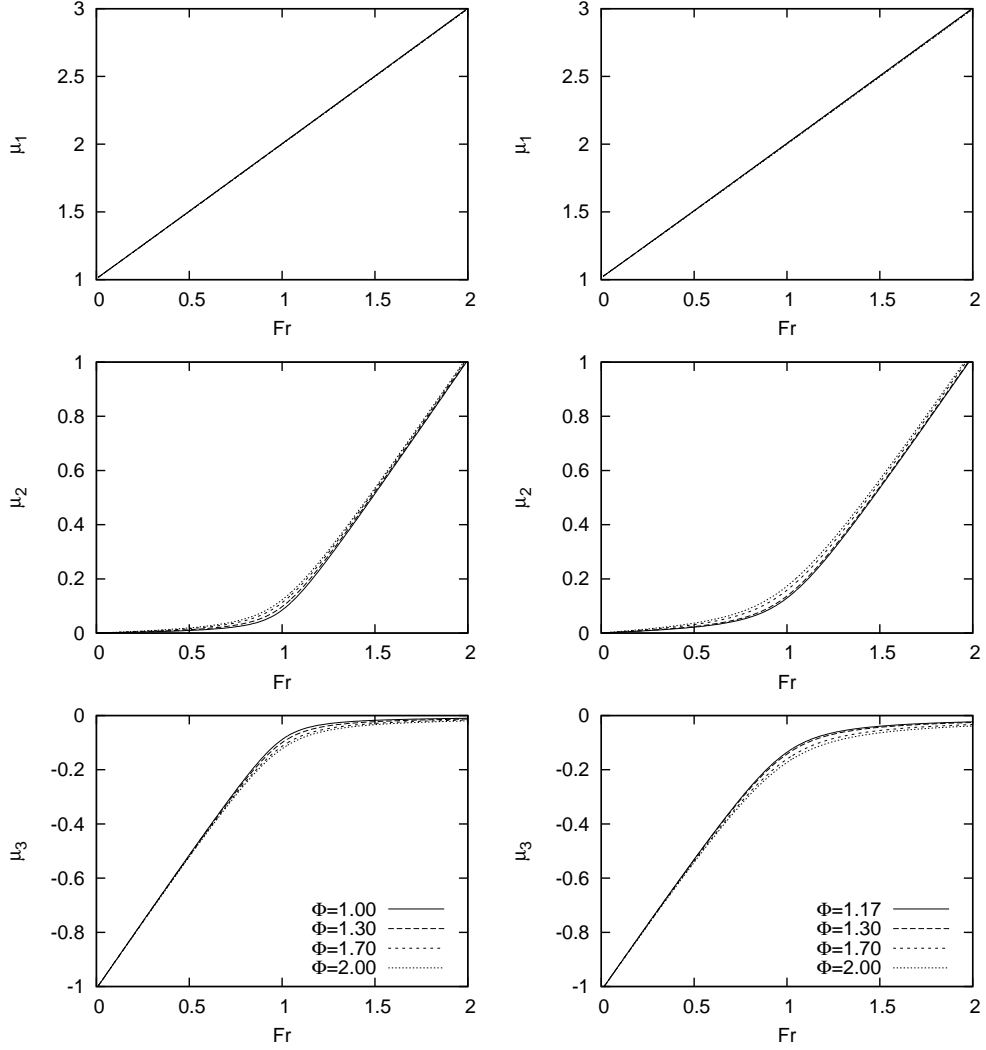
Figure 2: Eigenvalues of system (10) as functions of generalised Froude number, for different values of the shape parameter Φ and of the mobility parameter Θ for $\Psi = 5 \times 10^{-3}$. Eigenvalues for monomial transport formula ($\Theta = 1.00$) are presented in the left column, eigenvalues for Meyer–Peter and Müller transport formula with $\Theta = 2.00$ are presented in the right column. The rectangular cross section case is represented by $\Theta = 1.00$, $\Phi = 1.00$ and by $\Theta = 2.00$, $\Phi = 1.17$.

	$\Psi = 0.000$	$\Psi = 0.001$	$\Psi = 0.005$	$\Psi = 0.010$
$\Phi = 1.30$	0.00	0.14	0.13	0.13
$\Phi = 1.70$	0.00	0.29	0.28	0.28
$\Phi = 2.00$	0.00	0.40	0.39	0.37

Table 2: Relative variations of μ_3 at Fr = 1 for different values of Ψ and Φ with respect to the rectangular cross section case ($\Phi = 1.00$) with monomial transport formula ($\Theta = 1$).

	$\Psi = 0.000$	$\Psi = 0.001$	$\Psi = 0.005$	$\Psi = 0.010$
$\Phi = 1.30$	0.00	0.06	0.06	0.05
$\Phi = 1.70$	0.00	0.20	0.19	0.18
$\Phi = 2.00$	0.00	0.30	0.28	0.27

Table 3: Relative variations of μ_3 at Fr = 1 for different values of Ψ and Φ with respect to the rectangular cross section case ($\Phi = 1.17$) with Meyer–Peter and Müller transport formula and $\Theta = 2$.

the generalised Froude number (19) accounts for the cross section geometry and is to be used in the analysis of section–averaged model, instead of the classical Froude number which is based on the rectangular cross section geometry. The use of the traditional Froude number would indeed lead to an unphysical shift of the eigenvalues as functions of the Froude number.

In order to evaluate the dependency of the eigenstructure on the cross section geometry and on the transport formula, in figure 2 the eigenvalues calculated as functions of the generalised Froude number with $\Psi = 5 \times 10^{-3}$ are presented for different values of the shape parameter Φ and different transport formulae (i.e. different values of the mobility parameter Θ). While the first eigenvalue is almost unaffected by varying Φ and Θ, variations of the second and third eigenvalue are concentrated in a region around Fr = 1. The width of this region depends on the values of Φ and Θ: larger values of these parameters determine larger widths of this region.

In table 2 the relative variation of μ_3 at Fr = 1 with respect to the rectangular cross section case ($\Phi = 1$) are presented for the monomial transport formula ($\Theta = 1$) and different values of Φ and Ψ parameters. In table 3 the relative variations of μ_3 at Fr = 1 with respect to the rectangular cross section case with infinite surface width ($\Phi = 1.17$) are presented for Meyer–Peter and Müller transport formula with $\Theta = 2$ and different values of Φ and Ψ parameters (considering a rectangular cross section with an infinite surface width is equivalent to using a pure 1D model). It can be observed that the impact of the section shape on the eigenvalues (i.e. on the flow and sediment transport celerities) is quite large, so that significant errors can be expected if the details of the cross sections geometry are neglected.

5   Eigenvectors of the hyperbolic system for mobile–bed, free–surface channel flow

The left eigenvectors $\mathbf{L}_i$ associated with the non–dimensional eigenvalues μ_i of the hyperbolic system (10) can be expressed as functions of the generalised Froude number as follows:

$$\mathbf{L}_i = \left[-\frac{E_i}{D_i}, \, \frac{F_i}{D_i}, \, 1 \right] \tag{25}$$

where

$$
\begin{aligned}
D_i &= -\left(\mu_i + \mathrm{Fr}\right)^2, \tag{26} \\
E_i &= \mu_i^2 - \left(3\Theta\Phi\Psi + 2\right)\mathrm{Fr}\,\mu_i + 3\left(2\Phi - 1\right)\Theta\Psi\,\mathrm{Fr}, \tag{27} \\
F_i &= \sqrt{\frac{1}{gA_l}\frac{\partial A_l}{\partial \eta}}\left[-\left(3\Theta\Psi + 1\right)\mu_i + 3\Theta\Phi\Psi\,\mathrm{Fr}\right]. \tag{28}
\end{aligned}
$$

Here $i = 1, 2, 3$ and parameters Φ, Ψ and Θ are described in table 1. The complete derivation of the eigenvectors is reported in the appendix. The dimensions of F_i are $[(\mathrm{m\,s^{-1}})^{-1}]$, while D_i and E_i are non–dimensional quantities.

The following relation among left eigenvectors $\mathbf{L}_i$, dimensional and non–dimensional eigenvalues λ_i and μ_i respectively holds:

$$\mathbf{L}_i\mathbf{A} = \lambda_i\mathbf{L}_i\mathbf{B} = \mu_i\left(\frac{1}{gA_l}\frac{\partial A_l}{\partial \eta}\right)^{-1/2}\mathbf{L}_i\mathbf{B}, \qquad i = 1, 2, 3 \tag{29}$$

where $\mathbf{A}$ and $\mathbf{B}$ are the matrices of system (10). Using this relation it is possible to derive the canonical form of the system (see e.g. [20]). Multiplication of each term of equation (10) by $\mathbf{L}_i$ gives:

$$\mathbf{L}_i\mathbf{B}\frac{\partial \mathbf{U}}{\partial t} + \mathbf{L}_i\mathbf{A}\frac{\partial \mathbf{U}}{\partial x} = \mathbf{L}_i\mathbf{S}, \qquad i = 1, 2, 3. \tag{30}$$

Substitution of (29) into (30) gives:

$$\mathbf{L}_i\mathbf{B}\frac{\partial \mathbf{U}}{\partial t} + \mu_i\left(\frac{1}{gA_l}\frac{\partial A_l}{\partial \eta}\right)^{-1/2}\mathbf{L}_i\mathbf{B}\frac{\partial \mathbf{U}}{\partial x} = \mathbf{L}_i\mathbf{S}, \qquad i = 1, 2, 3. \tag{31}$$

Defining the material derivative:

$$\frac{D\mathbf{U}}{Dt}\bigg|_i = \frac{\partial \mathbf{U}}{\partial t} + \mu_i\left(\frac{1}{gA_l}\frac{\partial A_l}{\partial \eta}\right)^{-1/2}\frac{\partial \mathbf{U}}{\partial x}, \qquad i = 1, 2, 3, \tag{32}$$

it is possible to write the canonical form of system (10) as follows:

$$\mathbf{L}_i\mathbf{B}\,\frac{D\mathbf{U}}{Dt}\bigg|_i = \mathbf{L}_i\mathbf{S}, \qquad i = 1, 2, 3, \tag{33}$$

where

$$\mathbf{L}_i\mathbf{B} = \left[-\frac{E_i}{D_i}\frac{\partial A_l}{\partial \eta}, \, \frac{F_i}{D_i}, \, \frac{E_i}{D_i} + 1\right] \tag{34}$$

and the material derivative is evaluated along the characteristic curve defined by:

$$\frac{dx}{dt} = \lambda_i = \mu_i \left(\frac{1}{gA_l} \frac{\partial A_l}{\partial \eta} \right)^{-1/2} \tag{35}$$

Each of equations (33) is a weighted sum of rates of change of the primitive variables along the characteristic curve and this sum balances the source term (see e.g. the analysis in [18]). The primitive variables vary along the characteristic curves and the relative magnitude of their variations along the i–th curve is determined by the weights $\mathbf{L}_i\mathbf{B}$. Since equations (33) are in dimensional form, the quantitative comparison between the weights $\mathbf{L}_i\mathbf{B}$ is not straightforward. In order to compare the relative importance of each weight, however, it is possible to non–dimensionalise the canonical equation, rescaling lengths by a typical length H and velocities by a typical velocity C. This yields the following form of the canonical equation:

$$\widetilde{\mathbf{L}}_i\widetilde{\mathbf{B}} \left. \frac{D\widetilde{\mathbf{U}}}{Dt} \right|_i = \widetilde{\mathbf{L}}_i\widetilde{\mathbf{S}}, \qquad i = 1, 2, 3, \tag{36}$$

where

$$\widetilde{\mathbf{L}}_i\widetilde{\mathbf{B}} = \left[-\frac{E_i}{D_i} \frac{\partial \widetilde{A}_l}{\partial \widetilde{\eta}}, \ \frac{\widetilde{F}_i}{D_i}, \ \frac{E_i}{D_i} + 1 \right], \tag{37}$$

$$\widetilde{\mathbf{U}} = \left[\frac{\eta}{H}, \frac{Q_l}{H^2C}, \frac{A_s}{H^2} \right]^T, \tag{38}$$

$$\widetilde{\mathbf{S}} = \left[0, \frac{1}{HC^2} \frac{\bar{\tau}_0}{\rho} C_w \right]^T, \tag{39}$$

$$\widetilde{F}_i = -\left(\Psi + Q_l \frac{\partial \Psi}{\partial Q_l} + 1 \right) \mu_i + A_l \frac{\partial \Psi}{\partial A_s} \text{Fr}, \tag{40}$$

The quantity $\partial \widetilde{A}_l/\partial \widetilde{\eta}$ is equal to one for rectangular cross sections and increases for arbitrary cross sections; in particular, it can be very large when abrupt width changes occur.

6 Qualitative analysis of the different transport regimes

In this section, we will exploit the eigenstructure derived for system (10) to understand the behaviour of the system solutions in different transport regimes, as well as to investigate the strength of the coupling between liquid flow and sediment transport. We define the matrix of weights $\widetilde{\mathbf{L}}\widetilde{\mathbf{B}}$ in which the rows are given by the relation (37) for $i = 1, 2, 3$ and plot its components as functions of the generalised Froude number in different cases (figures 3–5). Graphs are composed in such a way that each row corresponds to a characteristic line. Thus the first column represents the weights of free surface variations, the second column the weights of liquid discharge variations and the third column the weights of solid area variations along

12
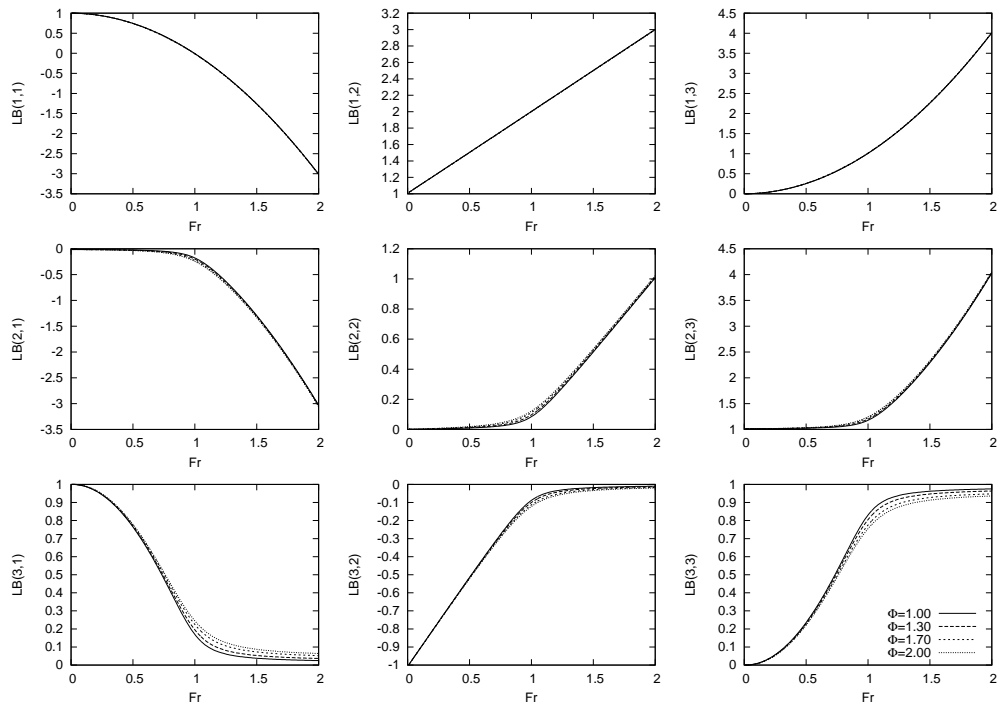
Figure 3: Non–dimensional weights $\widetilde{\mathbf{L}}\widetilde{\mathbf{B}}$ in equation (36) as functions of the generalised Froude number for $\Theta = 1.00$ (monomial transport formula), $\Psi = 5 \times 10^{-3}$, $\partial \widetilde{A}_l/\partial \widetilde{\eta} = 1.00$ and different values of the shape parameter Φ. The rectangular cross section case is represented by $\Phi = 1.00$.
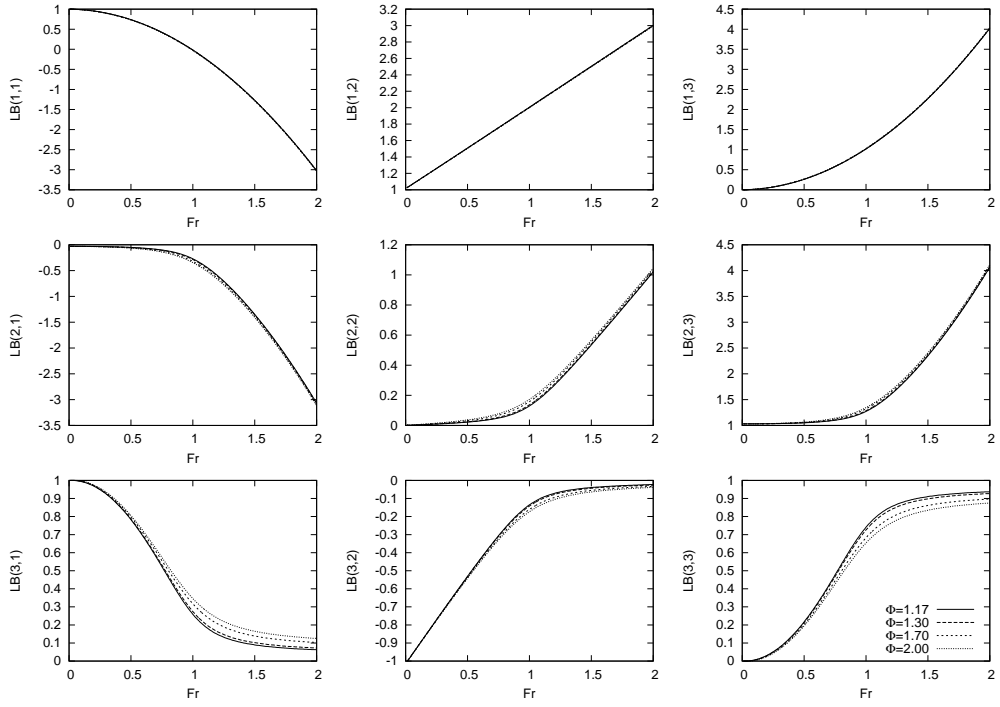
Figure 4: Non–dimensional weights $\widetilde{\mathbf{L}}\widetilde{\mathbf{B}}$ in equation (36) as functions of the generalised Froude number for $\Theta = 2.00$ (Meyer–Peter and Müller transport formula), $\Psi = 5 \times 10^{-3}$, $\partial \widetilde{A}_l / \partial \widetilde{\eta} = 1.00$ and different values of the shape parameter Φ. The rectangular cross section case is represented by $\Phi = 1.17$.

14
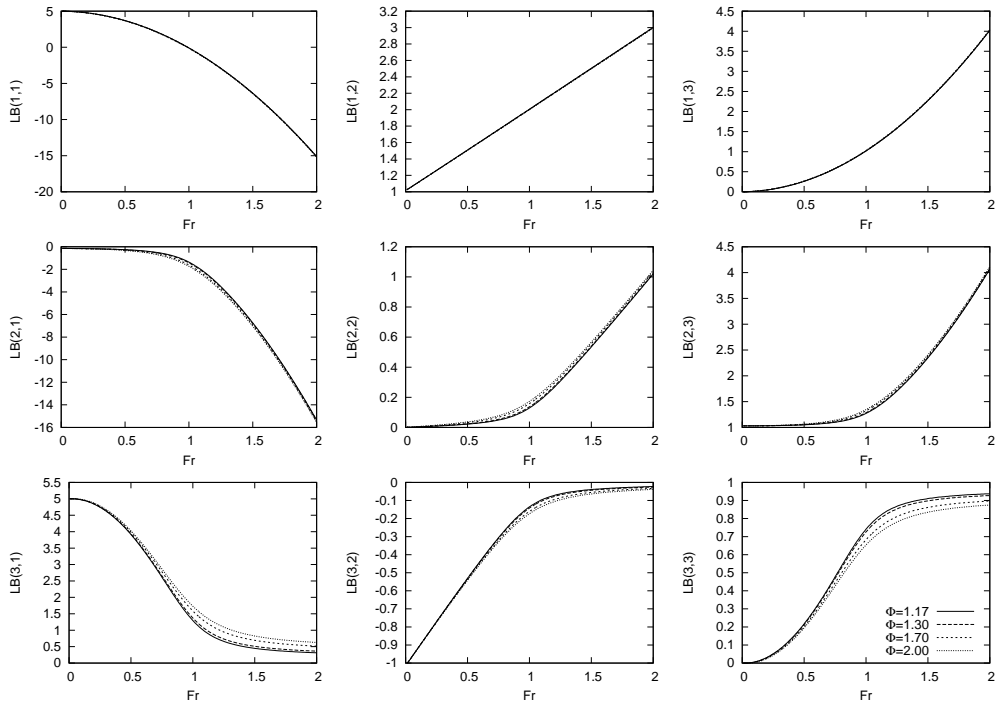
Figure 5: Non–dimensional weights $\widetilde{\mathbf{L}}\widetilde{\mathbf{B}}$ of the canonical equation (36) as functions of the generalised Froude number for $\Theta = 2.00$ (Meyer–Peter and Müller transport formula), $\Psi = 5 \times 10^{-3}$, $\partial \widetilde{A}_l / \partial \widetilde{\eta} = 5.00$ and different values of the shape parameter Φ.

each characteristic. In figures 3 and 4, $\partial \widetilde{A}_l / \partial \widetilde{\eta} = 1.00$ is considered, while in figure 5 $\partial \widetilde{A}_l / \partial \widetilde{\eta} = 5.00$ is considered.

The first and the second characteristics are associated to the positive eigenvalues μ_1 and μ_2, respectively, while the third characteristic is associated to the negative eigenvalue μ_3. Since $\mu_1 > \mu_2$, the first characteristic have a larger celerity. The variations of the weights at varying Φ and Θ are concentrated along the second and third characteristic (second and third line of each figure) in a region around Fr = 1. As noted before with the eigenvalues, the width of this region depends on the value of the non–dimensional parameters Φ, Ψ and Θ: larger values of these parameters make the width of the region larger.

For $\partial \widetilde{A}_l / \partial \widetilde{\eta} = 1.00$, along the first characteristic:

- for Fr $\ll$ 1 variations in solid area $\widetilde{A}_s$ are negligible with respect to variations in free surface elevation $\widetilde{\eta}$ and in liquid discharge $\widetilde{Q}_l$,

- for Fr $\simeq$ 1 variations in free surface elevation $\widetilde{\eta}$ are negligible with respect to variations in liquid discharge $\widetilde{Q}_l$ and in solid area $\widetilde{A}_s$,

- for Fr $\gg$ 1 all the variations have the same order of magnitude.

Along the second characteristic:

- for Fr $\ll$ 1 and for Fr $\simeq$ 1 variations in solid area $\widetilde{A}_s$ are dominant,

- for Fr $\gg$ 1 all the variations have the same order of magnitude.

Along the third characteristic:

- for Fr $\ll$ 1 variations in solid area $\widetilde{A}_s$ are negligible with respect to variations in free surface elevation $\widetilde{\eta}$ and in liquid discharge $\widetilde{Q}_l$,

- for Fr $\simeq$ 1 and for Fr $\gg$ 1 variations in solid area $\widetilde{A}_s$ are dominant.

For larger values of $\partial \widetilde{A}_l / \partial \widetilde{\eta}$, the range of variation of the weights associated to the free surface is larger than the others, so that free surface variations tend to dominate. n particular, for $\partial \widetilde{A}_l / \partial \widetilde{\eta} = 5.00$, along the first characteristic:

- for Fr $\ll$ 1 variations in free surface elevation $\widetilde{\eta}$ are dominant,

- for Fr $\simeq$ 1 variations in free surface elevation $\widetilde{\eta}$ are negligible with respect to variations in liquid discharge $\widetilde{Q}_l$ and in solid area $\widetilde{A}_s$,

- for Fr $\gg$ 1 variations in free surface elevation $\widetilde{\eta}$ are dominant.

Along the second characteristic:

- for Fr $\ll$ 1 variations in solid area $\widetilde{A}_s$ are dominant,

- for Fr $\simeq$ 1 variations in liquid discharge $\widetilde{Q}_l$ are negligible with respect to variations in free surface elevation $\widetilde{\eta}$ and in solid area $\widetilde{A}_s$,

- for Fr $\gg$ 1 variations in free surface elevation $\widetilde{\eta}$ are dominant.

Along the third characteristic:

- for Fr $\ll$ 1 variations in free surface elevation $\widetilde{\eta}$ are dominant,

- for Fr $\simeq$ 1 variations in liquid discharge $\widetilde{Q}_l$ are negligible with respect to variations in free surface elevation $\widetilde{\eta}$ and in solid area $\widetilde{A}_s$,

- for Fr $\gg$ 1 variations in solid area $\widetilde{A}_s$ are dominant.

Combining the information about the eigenvalues and the weights $\widetilde{\mathbf{L}}\widetilde{\mathbf{B}}$, it is possible to infer that for $\mathrm{Fr} \ll 1$ the perturbations of the free surface and of the liquid discharge travel downhill with celerity μ_1 along the first characteristic curve and uphill with celerity μ_3 along the third characteristic curve. The bed perturbation travels downhill on the second characteristic curve, whose celerity μ_2 is the smallest in absolute value. Hence, for $\mathrm{Fr} \ll 1$, the hydrodynamic processes and the morphodynamic processes are associated to distinct characteristic curves and the celerity of the latter is smaller, i.e. the evolution of the bed is quite slower than the evolution of the hydrodynamic variables η and Q_l. For $\mathrm{Fr} \simeq 1$ and $\mathrm{Fr} \gg 1$, on the contrary, there is no clear separation among the variations of the three variables, neither in terms of characteristic curves nor in terms of velocity of the evolution. It is worth noticing that for $\mathrm{Fr} > 1$ there is a significant component of A_s variation along the third characteristic curve; this explains why bed perturbations travel uphill for $\mathrm{Fr} > 1$.

Since for $\mathrm{Fr} \ll 1$ the variations of the hydrodynamic variables η and Q_l and the variations of the morphologic variable A_s travel on different characteristic curves, with different celerities, it seems natural to assume (see e.g. [19]) that in this regime the two processes can be considered decoupled, so that it would be possible to solve for the hydrodynamic variables at fixed bed and after that solving for the bed variations. The eigenvalues of the fixed–bed model are $\mu_i = \mathrm{Fr} \pm 1$, thus the ratio:

$$
r = \begin{cases}
\dfrac{\mu(3) - (\mathrm{Fr}-1)}{\mu(3)} & if \ \mathrm{Fr} < 1 \\[3mm]
\dfrac{\mu(2) - (\mathrm{Fr}-1)}{\mu(2)} & if \ \mathrm{Fr} \geq 1
\end{cases}
\tag{41}
$$

can be regarded as a measure of the strength of the coupling between hydrodynamic and morphodynamic processes. Indeed, for small values of r the eigenvalues of the fixed–bed and of the mobile–bed models are not too different. The values of r at different values of Φ, Ψ and Θ are presented in figures 6 and 7. The eigenvalues of the mobile–bed model are significantly different from those of the fixed–bed model in a region around $\mathrm{Fr} = 1$ but the width of this region depends on the values of the parameters Φ, Ψ and Θ. Particularly, for larger values of these parameters the width of this region is larger. It is also worth to notice that the region is not symmetrical around $\mathrm{Fr} = 1$. Sieben [19] analysed the eigenstructure of a one–dimensional model considering a monomial transport formula and suggested that the region in which the two processes should be considered coupled is $0.8 < \mathrm{Fr} < 1.2$; this bounds are commonly accepted in the literature (see e.g. [12]). The value r at $\mathrm{Fr} = 0.8$ and $\mathrm{Fr} = 1.2$ for the pure one–dimensional model with the monomial tranport formula ($\Phi = 1.00$, $\Theta = 1.00$) with $\Psi = 0.001$ are ~ 0.035. In figure 8 the values of Fr for which $r = 0.035$ are presented as a function of the shape parameter at different values of Ψ and Θ. It is then clear that the region in which relevant coupling takes place is strongly affected by the cross section geometry and by the nature and the intensity of sediment transport. As a consequence, it does not seem possible to define uniquely a decoupling region in the context of a realistic river flow model.

17
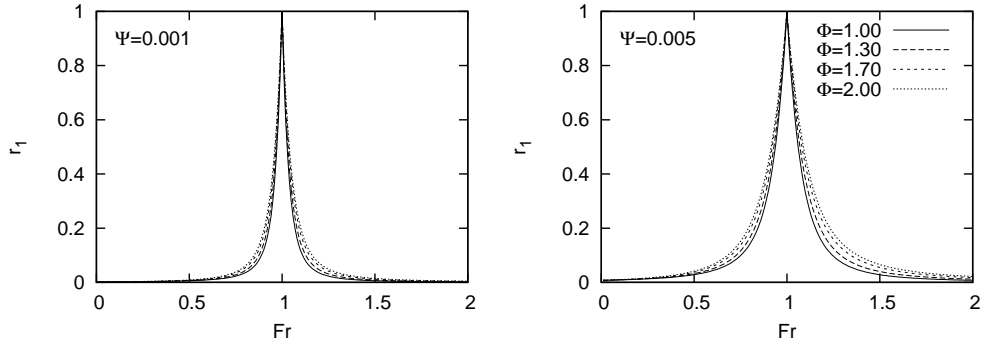
Figure 6: Values of the ratio r in equation (41) as a function of generalised Froude number for different values of Φ and Ψ and monomial formula ($\Theta = 1$).
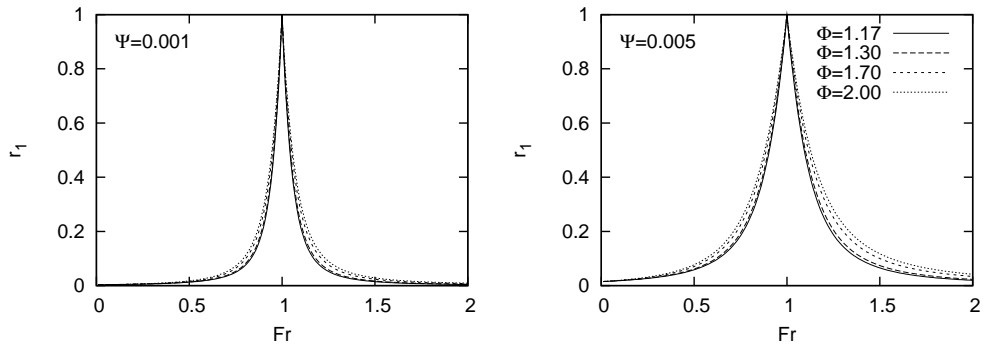
Figure 7: Values of the ratio r in equation (41) as a function of generalised Froude number for different values of Φ and Ψ and Meyer–Peter and Müller formula with $\Theta = 2$.
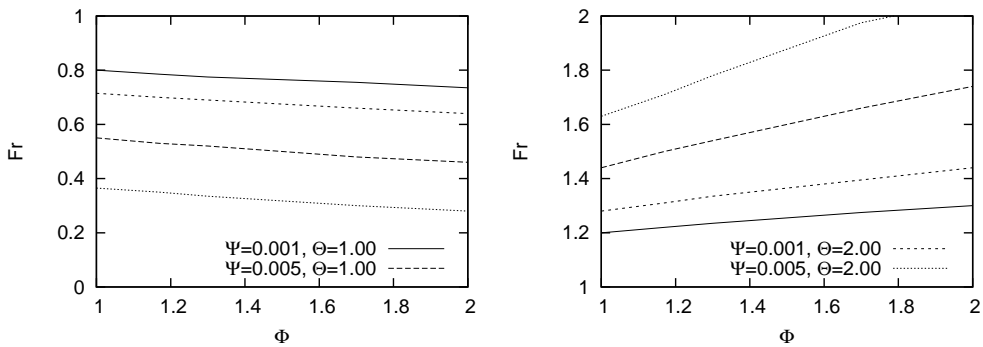
Figure 8: Values of Fr for which $r = 0.035$ as a function of the shape parameter Φ at different values of Ψ and Θ parameters.

Another clear consequence of the previous analysis is that the use of a one–dimensional model in cases of arbitrary cross sections can lead to large errors. However, it is still possible to define an equivalent rectangular cross section in which the equivalent width B_{eq} and the equivalent water depth h_{eq} are given by:

$$B_{eq} = \frac{\partial A_l}{\partial \eta}, \qquad h_{eq} = \frac{A_l}{B_{eq}} \qquad (42)$$

Assuming that the surface elevation η and the water discharge Q_l remain unchanged by the new geometry definition, relations (42) imply that $(A_l)_{eq} = A_l$, $U_{eq} = U$ and $(\mathrm{Fr})_{eq} = \mathrm{Fr}$, i.e. the flow regime is not affected by the new definition. Relations (42) do not guarantee that $(A_s)_{eq} = A_s$ but, provided that $\Psi_{eq} = \Psi$, the following holds: $\partial (A_s)_{eq}/\partial t = \partial A_s/\partial t$. For arbitrary cross sections $\partial A_l/\partial \eta$ is a function of η and, consequently, a function of time. The transport parameter Ψ depends, in general, on the shape of the cross section. Hence, a model using the rectangular cross section defined by (42) is equivalent to a section averaged model provided that the time variations of $\partial A_l/\partial \eta$ and the two–dimensional information related to the transport formula are accounted for.

7 Well posedness of hyperbolic systems for mobile–bed, free–surface channel flow

In this section, we study the well posedness of the mobile–bed system (10) as an initial and boundary value problem. Firstly, direct inspection of the system structure shows that the local existence and uniqueness results proven in [11] apply (see e.g. theorems 5.1.1, 5.1.2 therein). Thus, existence, uniqueness and regularity of a classical solution of system (10) are guaranteed for small perturbations of a stationary, constant solution. In particular, since it was shown in section 4 that $\lambda_1, \lambda_2 > 0$, $\lambda_3 < 0$, these results will hold on an interval $x \in [a, b]$ if the following boundary conditions are assigned at the left and right boundaries, respectively:

$$\begin{array}{rcll}
v_1(t) & = & G_1(t) & x = a \\
v_2(t) & = & G_2(t) & x = a \\
v_3(t) & = & G_3(t) & x = b.
\end{array} \qquad (43)$$

Here, $v_i = \mathbf{L}_i \mathbf{B} \mathbf{U}$ and G_i denote sufficiently regular functions of time. In general, these functions can also depend on the outgoing characteristics, but we do not consider this case in order to simplify the following well–posedness proof. Consider now the frozen coefficients, linearised system

$$\mathbf{B}\frac{\partial \mathbf{W}}{\partial t} + \mathbf{A}\frac{\partial \mathbf{W}}{\partial x} = 0, \qquad (44)$$

where $\mathbf{B}, \mathbf{A}$, are assumed to be constant matrices and $\mathbf{W}$ a perturbation of the state $\mathbf{U}$ around some constant reference solution. For simplicity, the friction terms have been neglected. It can be shown that, with an appropriate choice of the energy norm, energy inequalities can be derived

for the solution of (44) under the assumption that boundary conditions (43) hold. As a consequence, the frozen coefficients problem can be considered well posed according to the definition of Kreiss (see e.g. [9], [10]). Indeed, consider the positive definite matrix $\mathbf{R} = \sum_{i=1}^{3} \mathbf{B}^T \mathbf{L}_i^T \mathbf{L}_i \mathbf{B}$ and define the energy norm as

$$
\begin{aligned}
|||\mathbf{W}|||^2 \quad &= \int_a^b \mathbf{W}(x) \cdot \mathbf{R}\mathbf{W}(x)dx \\
&= \sum_{i=1}^{3} \int_a^b w_i^2(x)dx = \sum_{i=1}^{3} \int_a^b \mathbf{L}_i \mathbf{B}\mathbf{W}(x) \cdot \mathbf{L}_i \mathbf{B}\mathbf{W}(x)dx.
\end{aligned}
\tag{45}
$$

Here, $w_i = \mathbf{L}_i\mathbf{B}\mathbf{W}$ as in equation (43). Considering the energy norm variation in time and using equation (44) and the definition of the left eigenvalues, one yields

$$
\begin{aligned}
\frac{\partial}{\partial t}\frac{|||\mathbf{W}|||^2}{2} \quad &= \sum_{i=1}^{3} \int_a^b \mathbf{L}_i \mathbf{B}\mathbf{W}(x) \cdot \mathbf{L}_i \mathbf{B}\frac{\partial \mathbf{W}}{\partial t}(x)dx \\
&= -\sum_{i=1}^{3} \lambda_i \int_a^b \mathbf{L}_i \mathbf{B}\mathbf{W}(x) \cdot \mathbf{L}_i \mathbf{A}\frac{\partial \mathbf{W}}{\partial x}(x)dx \\
&= -\sum_{i=1}^{3} \frac{\lambda_i}{2} \int_a^b \frac{\partial}{\partial x}\left[\mathbf{L}_i \mathbf{B}\mathbf{W}(x) \cdot \mathbf{L}_i \mathbf{B}\mathbf{W}(x)\right]dx \\
&= \sum_{i=1}^{3} \frac{\lambda_i}{2}w_i^2(a) - \sum_{i=1}^{3} \frac{\lambda_i}{2}w_i^2(b).
\end{aligned}
\tag{46}\tag{47}
$$

Applying boundary conditions of type (43) to equation (44) and using the fact that $\lambda_1, \lambda_2 > 0$, $\lambda_3 < 0$, it follows that

$$
|||\mathbf{W}(t)|||^2 \leq |||\mathbf{W}(0)|||^2 + \frac{1}{2}\int_0^t \left[\lambda_1 G_1(s)^2 + \lambda_2 G_2(s)^2 - \lambda_3 G_3(s)^2\right]\ ds,
\tag{48}
$$

thus proving well posedness of system (44) in the sense of Kreiss.

8 Conclusions and perspectives for ongoing work

In this paper, the hyperbolic system associated to a section averaged sediment transport model has been analysed. The model, which allows for river sections of arbitrary shape, is a key component of state–of–the–art, realistic river flow modelling packages (see e.g. [21]). The eigenvalues and eigenvectors of the hyperbolic system have been expressed as functions of the generalised Froude number and of non dimensional parameters, related to the section shape and to the sediment transport regime. Appropriate boundary conditions have been derived, in order to achieve existence and uniqueness of classical solutions for small perturbations of steady state flows

and to guarantee the validity of an energy inequality for the linearised, frozen coefficient problem. On the basis of the eigenstructure analysis, the important issue of coupling between flow and morphological dynamics has been addressed, showing a strong dependency on the intensity and nature of the transport process and on the cross section shape.

Based on this work, efficient and accurate numerical methods for a section averaged sediment transport model will be investigated. In particular, in order to allow for long time range, high resolution realistic simulations at the lowest possible computational cost, the application of the time discretization techniques developed in [16] to the section averaged model equations will be studied, in the framework of the development of a mobile–bed, free–surface model based on the 1D–2D coupling technique proposed in [14],[15].

Appendix

Computation of the eigenvalues in the general case of mobile–bed channel flow

The characteristic polynomial of system (10) is given by:

$$p\left(\lambda\right) = \det\left(\mathbf{A} - \lambda\mathbf{B}\right) = a_3\lambda^3 + a_2\lambda^2 + a_1\lambda + a_0, \tag{49}$$

where:

$$
\begin{aligned}
a_0 &= \frac{Q_l^3}{A_l^2}\beta\frac{\partial\Psi}{\partial\eta} + \frac{Q_l^3}{A_l^2}\beta\frac{\partial\Psi}{\partial A_s}\frac{\partial A_l}{\partial\eta} - A_lQ_lg\frac{\partial\Psi}{\partial A_s} + \\
&\quad -\frac{Q_l^3}{A_l}\frac{\partial\Psi}{\partial A_s}\frac{\partial\beta}{\partial\eta} + \frac{Q_l^3}{A_l}\frac{\partial\Psi}{\partial\eta}\frac{\partial\beta}{\partial A_s},
\end{aligned} \tag{50}
$$

$$
\begin{aligned}
a_1 &= -\frac{Q_l^2}{A_l^2}\beta\frac{\partial A_l}{\partial\eta} + \frac{Q_l^2}{A_l}\frac{\partial\beta}{\partial\eta} + gA_l\left(1+\Psi\right) + \frac{Q_l^2}{A_l}\Psi\frac{\partial\beta}{\partial A_s}\frac{\partial A_l}{\partial\eta} + \\
&\quad +\frac{Q_l^2}{A_l}\Psi\frac{\partial\beta}{\partial\eta} - 2\frac{Q_l^2}{A_l}\beta\frac{\partial\Psi}{\partial A_s}\frac{\partial A_l}{\partial\eta} - 2\frac{Q_l^2}{A_l}\beta\frac{\partial\Psi}{\partial\eta} + \\
&\quad +\frac{Q_l^3}{A_l}\frac{\partial\beta}{\partial A_s}\frac{\partial\Psi}{\partial Q_l}\frac{\partial A_l}{\partial\eta} + \frac{Q_l^3}{A_l}\frac{\partial\beta}{\partial\eta}\frac{\partial\Psi}{\partial Q_l} + A_lQ_lg\frac{\partial\Psi}{\partial Q_l},
\end{aligned} \tag{51}
$$

$$a_2 = 2\frac{Q_l}{A_l}\beta\frac{\partial A_l}{\partial\eta} + Q_l\frac{\partial\Psi}{\partial A_s}\frac{\partial A_l}{\partial\eta} + Q_l\frac{\partial\Psi}{\partial\eta}, \tag{52}$$

$$a_3 = -\frac{\partial A_l}{\partial\eta}. \tag{53}$$

Rewriting the derivatives as follows

$$
\begin{aligned}
\frac{\partial\Psi}{\partial\eta} &= \frac{\partial\Psi}{\partial h}\frac{\partial h}{\partial\eta}, & \frac{\partial\Psi}{\partial A_s} &= \frac{\partial\Psi}{\partial h}\frac{\partial h}{\partial A_s}, \\
\frac{\partial A_l}{\partial\eta} &= \frac{\partial A_l}{\partial h}\frac{\partial h}{\partial\eta}, & \frac{\partial A_l}{\partial A_s} &= \frac{\partial A_l}{\partial h}\frac{\partial h}{\partial A_s} = -1, \\
\frac{\partial\beta}{\partial\eta} &= \frac{\partial\beta}{\partial h}\frac{\partial h}{\partial\eta}, & \frac{\partial\beta}{\partial A_s} &= \frac{\partial\beta}{\partial h}\frac{\partial h}{\partial A_s},
\end{aligned}
$$

it is possible to simplify (50)–(52):

$$a_0 = -A_l Q_l g \frac{\partial \Psi}{\partial A_s}, \tag{54}$$

$$a_1 = \frac{Q_l^2}{A_l^2} \left(A_l \frac{\partial \beta}{\partial \eta} - \beta \frac{\partial A_l}{\partial \eta} \right) + g A_l \left(1 + \Psi + Q_l \frac{\partial \Psi}{\partial Q_l} \right), \tag{55}$$

$$a_2 = 2\beta \frac{Q_l}{A_l} \frac{\partial A_l}{\partial \eta}. \tag{56}$$

After scaling by $\left[\left(-\frac{\partial A_l}{\partial \eta} \right)^{-1} \left(\frac{1}{g A_l} \frac{\partial A_l}{\partial \eta} \right)^{2/3} \right]$, the non–dimensional characteristic polynomial becomes:

$$p(\mu) = b_3 \mu^3 + b_2 \mu^2 + b_1 \mu + b_0, \tag{57}$$

where:

$$b_0 = A_l \frac{\partial \Psi}{\partial A_s} \, \mathrm{Fr}, \tag{58}$$

$$b_1 = \left[\beta - A_l \frac{\partial \beta}{\partial \eta} \left(\frac{\partial A_l}{\partial \eta} \right)^{-1} \right] \mathrm{Fr}^2 - \left(1 + \Psi + Q_l \frac{\partial \Psi}{\partial Q_l} \right), \tag{59}$$

$$b_2 = -2\beta \, \mathrm{Fr}, \tag{60}$$

$$b_3 = 1. \tag{61}$$

Here μ denotes the non–dimensional eigenvalues of equation (18) and Fr is the generalised Froude number defined in equation (19); both account for arbitrary cross section geometry.

We now consider the case in which Ψ is given by the monomial transport formula (11), the cross section is arbitrary and, for simplicity, $\beta = 1$. The derivative $\partial \Psi / \partial Q_l$ at fixed η and A_s is given by:

$$\frac{\partial \Psi}{\partial Q_l} = \frac{\partial}{\partial Q_l} \left(a_s \frac{Q_l^2}{A_l^2 h} \right) = \frac{2\Psi}{Q_l}. \tag{62}$$

The derivative $\partial \Psi / \partial A_s$ at fixed η and Q_l is given by:

$$\frac{\partial \Psi}{\partial A_s} = \frac{\partial}{\partial Q_l} \left(a_s \frac{Q_l^2}{A_l^2 h} \right) = \left(\frac{2}{A_l} - \frac{1}{h} \frac{\partial h}{\partial A_s} \right) \Psi. \tag{63}$$

Hence, the coefficients of the characteristic polynomial (57) are:

$$b_0 = \left(2 - \frac{A_l}{h} \frac{\partial h}{\partial A_s} \right) \Psi \, \mathrm{Fr}, \tag{64}$$

$$b_1 = \mathrm{Fr}^2 - 1 - 3\Psi, \tag{65}$$

$$b_2 = -2 \, \mathrm{Fr}, \tag{66}$$

$$b_3 = 1. \tag{67}$$

It is now possible to rewrite coefficient b_0 as:

$$b_0 = 3\Phi \Psi \, \mathrm{Fr}, \tag{68}$$

where the shape parameter Φ is defined by:

$$\Phi = \frac{1}{3}\left(2 - \frac{A_l}{h}\frac{\partial h}{\partial A_s}\right). \tag{69}$$

In the case of rectangular cross section $A_l = Bh$ and $\partial h/\partial A_s = -1/B$, hence $\Phi = 1$.

Alternatively, we can consider Ψ as given by the Meyer–Peter and Müller formula (17), along with an arbitrary cross section and, for simplicity, $\beta = 1$. The Shields mobility parameter θ is defined in equation (12) and depends on the Chézy roughness coefficient χ. In general cases, the Chézy coefficient is non–constant; its dependency on the hydraulic radius $R_h = A_l/C_w$ is given by the Strickler formula:

$$\chi = KR_h^{1/6}, \tag{70}$$

where K is the Strickler roughness coefficient.

In the case $\theta \leq \theta_c$, Ψ and its derivatives are zero and the fixed–bed case is recovered. In the more interesting case $\theta > \theta_c$, the derivative $\partial \Psi/\partial Q_l$ at fixed η and A_s is:

$$\frac{\partial \Psi}{\partial Q_l} = \frac{\partial}{\partial Q_l}\left(\frac{Q_s}{Q_l}\right) = \frac{1}{Q_l}\left(\frac{\partial Q_s}{\partial Q_l} - \Psi\right). \tag{71}$$

The derivative $\partial Q_s/\partial Q_l$ at fixed η and A_s is:

$$\frac{\partial Q_s}{\partial Q_l} = \frac{\partial}{\partial Q_l}\left(8Bd\sqrt{gd\Delta}\left(\theta - \theta_c\right)^{3/2}\right) = \frac{3}{2}\frac{Q_s}{\theta - \theta_c}\frac{\partial \theta}{\partial Q_l}. \tag{72}$$

Using the definitions of θ and χ yields:

$$\frac{\partial \theta}{\partial Q_l} = \frac{\partial}{\partial Q_l}\left(\frac{Q_l^2}{A_l^2\chi^2 d\Delta}\right) = \frac{2\theta}{Q_l}. \tag{73}$$

Substitution of (73) and (72) in (71) yields:

$$\frac{\partial \Psi}{\partial Q_l} = \frac{\Psi}{Q_l}\left(3\frac{\theta}{\theta - \theta_c} - 1\right). \tag{74}$$

The derivative $\partial \Psi/\partial A_s$ at fixed η and Q_l is:

$$\frac{\partial \Psi}{\partial A_s} = \frac{\partial}{\partial A_s}\left(\frac{Q_s}{Q_l}\right) = \frac{1}{Q_l}\left(\frac{\partial Q_s}{\partial A_s}\right). \tag{75}$$

The derivative $\partial Q_s/\partial A_s$ at fixed η and Q_l is:

$$\frac{\partial Q_s}{\partial A_s} = \frac{\partial}{\partial A_s}\left(8Bd\sqrt{gd\Delta}\left(\theta - \theta_c\right)^{3/2}\right) = \frac{3}{2}\frac{Q_s}{\theta - \theta_c}\frac{\partial \theta}{\partial A_s}. \tag{76}$$

The derivative $\partial \theta/\partial A_s$ at fixed η and Q_l is:

$$\frac{\partial \theta}{\partial A_s} = \frac{\partial}{\partial A_s}\left(\frac{Q_l^2}{A_l^2\chi^2 d\Delta}\right) = 2\theta\left(\frac{1}{A_l} - \frac{1}{\chi}\frac{\partial \chi}{\partial A_s}\right).$$

The derivative $\partial\chi/\partial A_s$ at fixed η and Q_l is:

$$\frac{\partial\chi}{\partial A_s} = \frac{\partial}{\partial A_s}\left(KR_h^{1/6}\right) = \frac{K}{6}R_h^{-5/6}\frac{\partial R_h}{\partial h}\frac{\partial h}{\partial A_s}. \tag{77}$$

Substitution of (70) and (76)–(77) in (75) yields:

$$\frac{\partial\Psi}{\partial A_s} = 3\Psi\frac{\theta}{\theta-\theta_c}\frac{1}{A_l}\left[1-\frac{C_w}{6}\frac{\partial R_h}{\partial h}\frac{\partial h}{\partial A_s}\right]. \tag{78}$$

Hence, the coefficients of the characteristic polynomial (57) are:

$$b_0 = 3\frac{\theta}{\theta-\theta_c}\left[1-\frac{C_w}{6}\frac{\partial R_h}{\partial h}\frac{\partial h}{\partial A_s}\right]\Psi\,\mathrm{Fr}, \tag{79}$$

$$b_1 = \mathrm{Fr}^2 - 1 - 3\frac{\theta}{\theta-\theta_c}\Psi, \tag{80}$$

$$b_2 = -2\,\mathrm{Fr}, \tag{81}$$

$$b_3 = 1. \tag{82}$$

It is now possible to rewrite coefficients b_0 and b_1 as:

$$b_0 = 3\Theta\Phi\Psi\,\mathrm{Fr}, \tag{83}$$

$$b_1 = \mathrm{Fr}^2 - 1 - 3\Theta\Psi, \tag{84}$$

where the shape parameter Φ is defined by:

$$\Phi = \left[1-\frac{C_w}{6}\frac{\partial R_h}{\partial h}\frac{\partial h}{\partial A_s}\right] \tag{85}$$

and the mobility parameter Θ is defined by:

$$\Theta = \frac{\theta}{\theta-\theta_c}. \tag{86}$$

In the case of rectangular cross section $C_w = B + 2h$, $R_h = \frac{Bh}{B+2h}$, hence $\frac{\partial R_h}{\partial h} = \frac{B^2}{(B+2h)^2}$ and $\Phi = \left[1-\frac{B}{6(B+2h)}\right]$. From the calculation presented here, it is clear that the system eigenstructure can be described by the general formula (20) with coefficients given by (21)–(24) and summarised in table 1.

Computation of the eigenvectors in the general case of mobile–bed channel flow

The left eigenvectors $\mathbf{L}_i$ associated with the dimensional eigenvalues λ_i of the hyperbolic system (10) are computed by solving $\mathbf{L}_i(\mathbf{A} - \lambda_i\mathbf{B}) = \mathbf{0}$. Since only two equations are linearly independent, the system has infinite solutions. Using the second and the third equation and considering vectors of the form $[(L_1)_i, (L_2)_i, 1]$, the following expressions can be found:

$$(L_1)_i = -\frac{E_i}{D_i}, \qquad (L_1)_i = \frac{F_i}{D_i}, \tag{87}$$

where

$$D_i = A_l^2 \frac{\partial A_l}{\partial A_s} \lambda_i^2 - 2 A_l Q_l \beta \frac{\partial A_l}{\partial A_s} \lambda_i + Q_l^2 \left(\beta \frac{\partial A_l}{\partial A_s} - A_l \frac{\partial \beta}{\partial A_s} \right), \quad (88)$$

$$E_i = A_l^2 \lambda_i^2 - Q_l A_l \left(A_l \frac{\partial \Psi}{\partial A_s} + 2\beta \right) \lambda_i +$$
$$+ Q_l^2 \left[\left(\Psi + Q_l \frac{\partial \Psi}{\partial Q_l} \right) \left(\beta \frac{\partial A_l}{\partial A_s} - A_l \frac{\partial \beta}{\partial A_s} \right) + 2 A_l \beta \frac{\partial \Psi}{\partial A_s} \right], \quad (89)$$

$$F_i = A_l^2 \left[\frac{\partial A_l}{\partial A_s} \left(\Psi + Q_l \frac{\partial \Psi}{\partial Q_l} \right) - 1 \right] \lambda_i + A_l^2 Q_l \frac{\partial \Psi}{\partial A_s}, \quad (90)$$

and $i = 1, 2, 3$. Assuming $\beta = 1$ and $\partial A_l / \partial A_s = -1$ as explained in section 2 and rescaling D_i, E_i and F_i by a factor $\left(\frac{1}{g A_l} \frac{\partial A_l}{\partial \eta} \right)$ (which is equivalent to multiplying and dividing each component of $\mathbf{L}_i$ by the same factor) gives the left eigenvectors associated with the non–dimensional eigenvalues μ_i as functions of the generalised Froude number:

$$D_i = -(\mu_i + \text{Fr})^2, \quad (91)$$

$$E_i = \mu_i^2 - \left(A_l \frac{\partial \Psi}{\partial A_s} + 2 \right) \text{Fr} \, \mu_i +$$
$$+ \left[2 A_l \frac{\partial \Psi}{\partial A_s} - \left(\Psi + Q_l \frac{\partial \Psi}{\partial Q_l} \right) \right] \text{Fr}^2, \quad (92)$$

$$F_i = \sqrt{\frac{1}{g A_l} \frac{\partial A_l}{\partial \eta}} \left[-\left(\Psi + Q_l \frac{\partial \Psi}{\partial Q_l} + 1 \right) \mu_i + A_l \frac{\partial \Psi}{\partial A_s} \text{Fr} \right]. \quad (93)$$

Computing the derivatives of Ψ for different transport formulae and different geometries, as done previously for the computation of the eigenvalues, and using the parameters Φ, Ψ and Θ described in table 1, it is possible to rewrite (91)–(93) in the form presented in relations (26)–(28).

Acknowledgements

References

[1] A. Armanini. *Principi di idraulica fluviale.* Editoriale Bios, Cosenza, 1999.

[2] C.B. Brown. *Engineering Hydraulics*, chapter XII Sediment Transportation, pages 769–857. John Wiley, 1950.

[3] H. Capart, T.I Heldo, S.Y. Huang, D.L. Young, and Y. Zech. Treatment of natural geometries in finite volume river flow computations. *ASCE Journal of Hydraulic Engineering*, 129:385–393, 2003.

[4] M. de Vries. Considerations about non–steady bed–load transport in open channels. *Proc. XI IAHR Congr.*, pages 3.8.1–3.8.8, 1965.

[5] M.J. Castro Diaz, E.D. Fernandez Nieto, and A. M. Ferreiro. Some well balanced shallow water sediment transport models. In A. Bermudez de Castro et al., editor, *Numerical Mathematics and Advanced Applications.*, pages 292–315. Springer Verlag, ENUMATH2005, 2006.

[6] H.A. Einstein. The Bed–Load Function for Sediment Trasnsportation in Open Channel Flow. *Technical Bulletin No. 1026, Dept. of Agriculture, Washington D.C.*, 1950.

[7] F. Engelund and E. Hansen. *A monograph on sediment transport in alluvial stream.* Teknisk Forlag, Copenhagen, Denmark, 1967.

[8] J. Hudson and P.K. Sweby. Formulations for numerically approximating hyperbolic systems governing sediment transport. *Journal of Scientific Computing*, 19:225–252, 2003.

[9] H.O. Kreiss. Initial Boundary Value Problems for Hyperbolic Systems. *Communications on Pure and Applied Mathematics*, 22:277–298, 1970.

[10] H.O. Kreiss and J. Lorenz. *Initial-Boundary Value Problems and the Navier–Stokes Equations.* Academic Press, 1989.

[11] T.T. Li. *Global classical solutions for quasilinear hyperbolic systems.* Wiley — Masson, 1994.

[12] D.A. Lyn and M. Altinakar. St. Venant–Exner Equations for Near–Critical and Transcritical Flows. *ASCE Journal of Hydraulic Engineering*, 128(6):579–587, 2002.

[13] E. Meyer-Peter and R. Müller. Formulas for bed–load transport. *Proc. 2nd Meeting IAHSR, Stockholm, Sweden*, pages 1–26, 1948.

[14] E. Miglio, S. Perotto, and F. Saleri. Model coupling techniques for free–surface flow problems: Part I. *Nonlinear Analysis*, 63:1885–1896, 2005.

[15] E. Miglio, S. Perotto, and F. Saleri. Model coupling techniques for free–surface flow problems: Part II. *Nonlinear Analysis*, 63:1897–1908, 2005.

[16] E. Miglio, A. Quarteroni, and F. Saleri. Finite element approximation of quasi–3d shallow water equations. *Computer Methods in Applied Mechanics and Engineering*, 174:355–369, 1999.

[17] G. Parker. Surface–based bedload transport relation for gravel rivers. *Journal of Hydraulic Research*, 28(4):417–436, 1990.

[18] G. Rosatti and L. Fraccarollo. A well–balanced approach for flows over mobile–bed with high sediment–transport. *Journal of Computational Physics*, 220(1):312–338, 2006.

[19] J. Sieben. A theoretical analysis of discontinuous flows with mobile bed. *Journal of Hydraulic Research*, 37(2):199–212, 1999.

[20] E.F. Toro. *Riemann solvers and numerical methods for fluid dynamics.* Springer–Verlag, 1997.

[21] W. Wu and D. Vieira. One Dimensional Channel Network Model. *Technical Report NCCHE-TR-2002-1, National Center for Computational Hydroscience and Engineering, University of Mississippi*, 2002.